ALIEN EARTHS

EARTHS IN OTHER SOLAR SYSTEMS

Recent Publications

Jupiter as an Exoplanet: Insights from Cassini Phase Curves

.....

Evidence for an MHD disk wind via optical forbidden line spectro-astrometry

.....

ACCESS: An optical transmission spectrum of the high-gravity, hot Jupiter HAT-P-23b

.....

A stellar mass dependence of structured disks: a possible link with exoplanet demographics

.....

A deuterium-poor water reservoir in the asteroid 4 Vesta and the inner solar system

.....

Lithologic Controls on Silicate Weathering Regimes of Temperate Planets

.....

Thresholds for Particle Clumping by the Streaming Instability

.....

System-level fractionation of carbon from disk and planetesimal processing

.....

Earths in Other Solar Systems and Alien Earths are part of NASA's Nexus for Exoplanetary System Science program, which carries out coordinated research toward the goal of searching for and determining the frequency of habitable extrasolar planets with atmospheric biosignatures in the Solar neighborhood.

Our interdisciplinary teams includes astrophysicists, planetary scientists, cosmochemists, material scientists, chemists, biologists, and physicists.

The Principal Investigator of Project EOS and Alien Earths is Daniel Apai (University of Arizona). The projects' lead institutions are The University of Arizona's Steward Observatory and Lunar and Planetary Laboratory.

For a complete list of publications, please visit the **EOS Library** and **AE Library** on the SAO/NASA Astrophysics Data System.

ALIEN EARTHS | EARTHS IN OTHER SOLAR SYSTEMS

Origins Seminar

The **Origins Seminar** series brings together ISM, star and planet formation people, exoplanets experts, planetary scientists and astrobiologists. Topics range from molecular clouds through star and planet formation to exoplanets detection and characterization and astrobiology.

The seminar series is organized by Serena Kim (SO), Kamber Schwarz (LPL), Sebastiaan Krijt (University of Exeter, UK) and Sebastiaan Haffert (SO) from Steward Observatory/Dept. of Astronomy and Dept. of Planetary Sciences (LPL) at the University of Arizona. The Origins Seminar series is partly supported by the Earths in Other Solar Systems NExSS team.

Talks take place **12:00 – 1:00pm (MST) on Mondays**. To receive weekly updates and advertisements for talks, please subscribe to the **mailing list**. If you are interested in presenting your work during one of the open slots, feel free to contact **the organizers**.

Currently, the Origins seminar meets via Zoom due to the Covid-19 Pandemic. We may continue to meet via zoom through Summer 2021, depending on the status of the Pandemic and guidelines by the department and the University. The Zoom information is sent via email.

Origins Seminars YouTube Channel

ALIEN EARTHS | EARTHS IN OTHER SOLAR SYSTEMS

Alien Earths Website

The Alien Earths website has launched! We are in the process of updating content and adding images, and would greatly appreciate your input. Please send your suggestions via the Alien Earths “website” Slack channel. Thank you!

Jupiter as an Exoplanet: Insights from Cassini Phase Curves

Kevin Heng and Liming Li

The Astrophysical Journal Letters, Volume 909, Issue 2

Due to its proximity to Earth, Jupiter of the solar system serves as a unique case study for gas-giant exoplanets. In the current Letter, we perform fits of ab initio, reflective, semi-infinite, homogeneous model atmospheres to 61 phase curves from 0.40 to 1.00 μm, obtained from the Cassini spacecraft, within a Bayesian framework. We reproduce the previous finding that atmospheric models using classic reflection laws (Lambertian, Rayleigh, single Henyey-Greenstein) provide poor fits to the data. Using the double Henyey-Greenstein reflection law, we extract posterior distributions of the single-scattering albedo and scattering asymmetry factors and tabulate their median values and uncertainties. We infer that the aerosols in the Jovian atmosphere are large, irregular, polydisperse particles that produce strong forward scattering together with a narrow backscattering lobe. The near-unity values of the single-scattering albedos imply that multiple scattering of radiation is an important effect. We speculate that the observed narrow backscattering lobe is caused by coherent backscattering of radiation, which is usually associated with solar system bodies with solid surfaces and regolith. Our findings demonstrate that precise, multiwavelength phase curves encode valuable information on the fundamental properties of cloud/haze particles. The method described in this Letter enables single-scattering albedos and scattering asymmetry factors to be retrieved from James Webb Space Telescope phase curves of exoplanets.

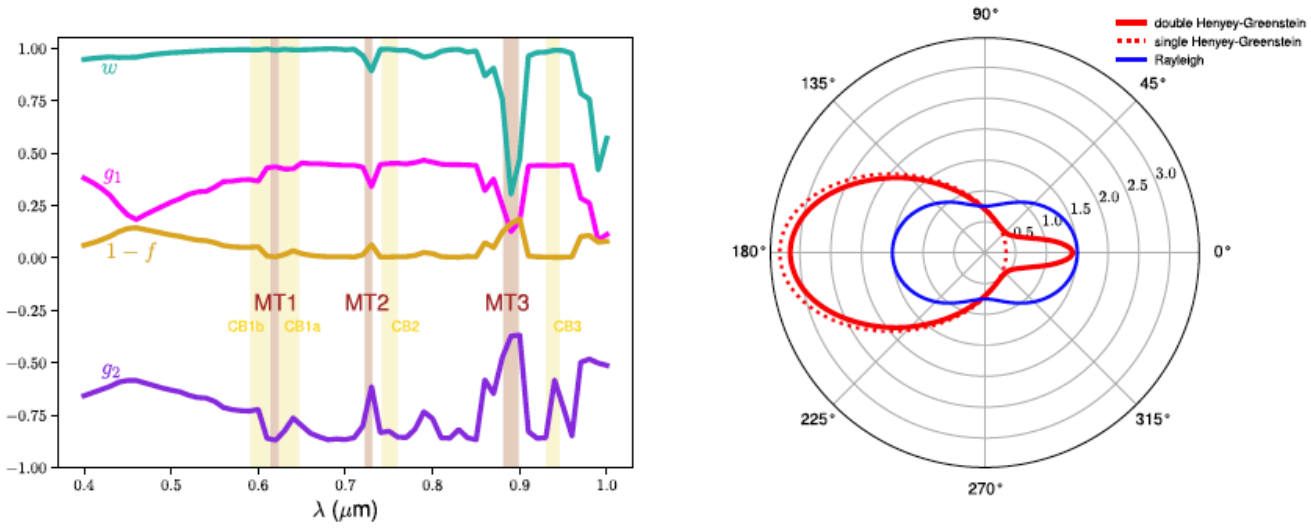

Figure 3. The left panel shows the inferred DHG parameters: single-scattering albedo ω, scattering asymmetry factors g_1 and g_2, and weighting factor $1 - f$. Inferred uncertainties on the parameters are not shown as they are typically smaller than the width of the line. The right panel shows visualizations of the single Henyey–Greenstein (adopting a mean value of $\bar{g}_1 = 0.36$), double Henyey–Greenstein (adopting mean values of $\bar{g}_1 = 0.36$, $\bar{g}_2 = -0.71$ and $\bar{f} = 0.95$), and Rayleigh scattering phase functions. Isotropic scattering is represented by a unit circle (not shown). Angles stated are the values of $\alpha = 180° - \beta$ with β being the scattering angle. Generally, the particles simultaneously exhibit strong forward scattering ($f \sim 1$) and a narrow backscattering lobe. The MT1 (0.615–0.623 μm), MT2 (0.723–0.730 μm), and MT3 (0.882–0.898 μm) methane absorption bands (Porco et al. 2004) are indicated with translucent bars. The corresponding continuum bands are CT1b (0.592–0.612 μm), CT1a (0.625–0.646 μm), CT2 (0.743–0.759 μm), and CT3 (0.931–0.945 μm), which are also indicated with translucent bars.

Evidence for an MHD disk wind via optical forbidden line spectro-astrometry

Whelan, E. T; Pascucci, I.; Gorti, U.; Edwards, S.; Alexander, R. D.; Sterzik, M. F.; Melo, C.

Accepted for publication in The Astrophysical Journal

Spectro-astrometry is used to investigate the low velocity component (LVC) of the optical forbidden emission from the T Tauri stars RU Lupi and AS 205 N. Both stars also have high velocity forbidden emission (HVC) which is tracing a jet. For AS 205 N, analysis reveals a complicated outflow system. For RU Lupi, the [O I] 6300 and [S II] 6716, 6731 LV narrow component (NC) is offset along the same position angle (PA) as the HVC but with a different velocity gradient than the jet, in that displacement from the stellar position along the rotation axis is decreasing with increasing velocity. From the LVC NC PA and velocity gradient, it is inferred that the NC is tracing a wide angled MHD disk wind. A photoevaporative wind is ruled out. This is supported by a comparison with a previous spectro-astrometric study of the CO fundamental line. The decrease in offset with increasing velocity is interpreted as tracing an increase in the height of the wind with increasing disk radius. This is one of the first measurements of the spatial extent of the forbidden emission line LVC NC (~ 40 au, 8 au for RU~Lupi in the [S II] 6731 and [O I] 6300 lines) and the first direct confirmation that the LVC narrow component can trace an MHD disk wind.

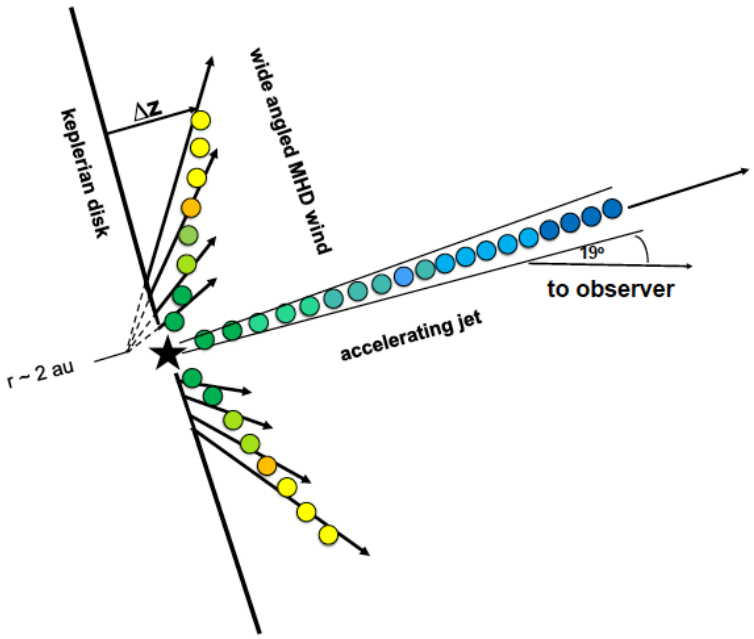

Figure 10. Sketch illustrating how the spectro-astrometric signals presented in Figures 1 and 2 are tracing the outflows from RU Lupi. The coloured dots are the positional displacements shown in Figure 2 with the colors from yellow (0 km/s) to dark blue (-230 km/s) representing increasing velocities. The HVC2 is tracing the accelerating jet with velocities from -90 km/s to -230 km/s. The LVC NC is tracing a wide angled MHD disk wind with a velocity range of -40 km/s to 0 km/s. For the MHD wind component, the velocity of each point corresponds to flow streamline and therefore a disk radius r. The spectro-astrometric technique is recording the height of the emission above the disk z, at each velocity (or r). As the velocity is decreasing with increasing r and z is increasing with r, the spectro-astrometric results shown in Figure 2 for the NC, has a negative velocity gradient.

ACCESS: An optical transmission spectrum of the high-gravity, hot Jupiter HAT-P-23b

Weaver, Ian C. ; López-Morales, Mercedes ; Alam, Munazza K. ; Espinoza, Néstor ; Rackham, Benjamin V. ; Goyal, Jayesh M. ; MacDonald, Ryan J. ; Lewis, Nikole K. ; Apai, Dániel ; Bixel, Alex ; Jordán, Andrés ; Kirk, James ; McGruder, Chima ; Osip, David J.

Accepted for publication in The Astronomical Journal

We present a new ground-based visible transmission spectrum of the high-gravity, hot Jupiter HAT-P-23b, obtained as part of the ACCESS project. We derive the spectrum from five transits observed between 2016 and 2018, with combined wavelength coverage between 5200 Å - 9269 Å in 200 Å bins, and with a median precision of 247 ppm per bin. HAT-P-23b's relatively high surface gravity (g ~ 30 m/s^2), combined with updated stellar and planetary parameters from Gaia DR2, gives a 5-scale-height signal of 384 ppm for a hydrogen-dominated atmosphere. Bayesian models favor a clear atmosphere for the planet with the tentative presence of TiO, after simultaneously modeling stellar contamination, using spots parameter constraints from photometry. If confirmed, HAT-P-23b would be the first example of a high-gravity gas giant with a clear atmosphere observed in transmission at optical/NIR wavelengths; therefore, we recommend expanding observations to the UV and IR to confirm our results and further characterize this planet. This result demonstrates how combining transmission spectroscopy of exoplanet atmospheres with long-term photometric monitoring of the host stars can help disentangle the exoplanet and stellar activity signals.

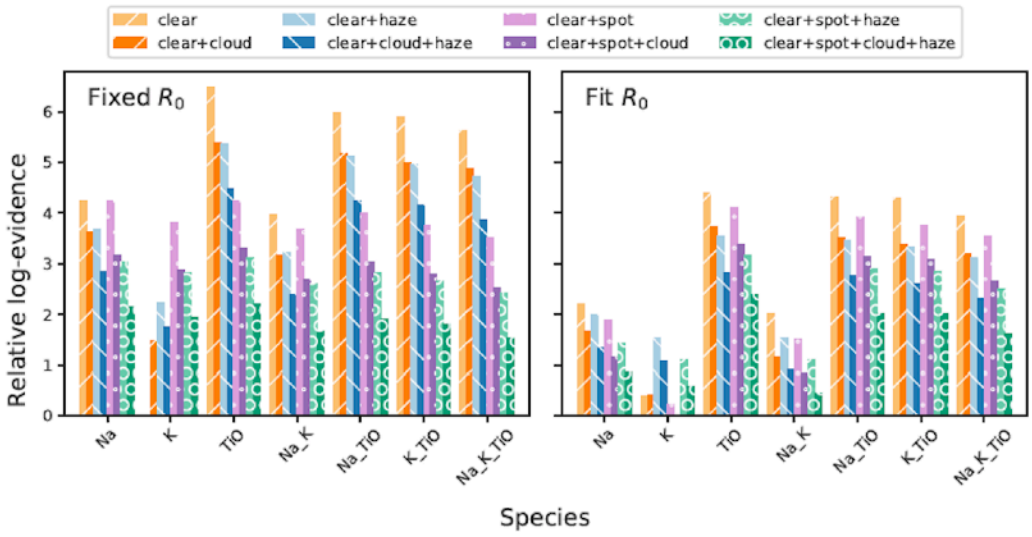

Figure 7. Representative summary of Bayesian log-evidences of retrieved models relative to the model with the lowest log-evidence (left: Fixed R0, K, clear; right: Fit R_0, K, clear+spot+cloud). Both sets correspond to ($T_{sp,lower}$; $f_{sp,lower}$) = (2;200K; 0:022), with R_0 = 12,966 ppm fixed to our observed mean white-light curve depth in the left panel. A trend can be seen favoring models with TiO present in the planet's atmosphere over contributions originating from stellar activity. (</>)

A stellar mass dependence of structured disks: a possible link with exoplanet demographics

van der Marel, Nienke; Mulders, Gijs

Accepted for publication in The Astrophysical Journal

Gaps in protoplanetary disks have long been hailed as signposts of planet formation. However, a direct link between exoplanets and disks remains hard to identify. We present a large sample study of ALMA disk surveys of nearby star-forming regions to disentangle this connection. All disks are classified as either structured (transition, ring, extended) or non-structured (compact) disks. Although low-resolution observations may not identify large scale substructure, we assume that an extended disk must contain substructure from a dust evolution argument. A comparison across ages reveals that structured disks retain high dust masses up to at least 10 Myr, whereas the dust mass of compact, non-structured disks decreases over time. This can be understood if the dust mass evolves primarily by radial drift, unless drift is prevented by pressure bumps. We identify a stellar mass dependence of the fraction of structured disks. We propose a scenario linking this dependence with that of giant exoplanet occurrence rates. We show that there are enough exoplanets to account for the observed disk structures if transitional disks are created by exoplanets more massive than Jupiter, and ring disks by exoplanets more massive than Neptune, under the assumption that most of those planets eventually migrate inwards. On the other hand, the known anti-correlation between transiting super-Earths and stellar mass implies those planets must form in the disks without observed structure, consistent with formation through pebble accretion in drift-dominated disks. These findings support an evolutionary scenario where the early formation of giant planets determines the disk's dust evolution and its observational appearance.

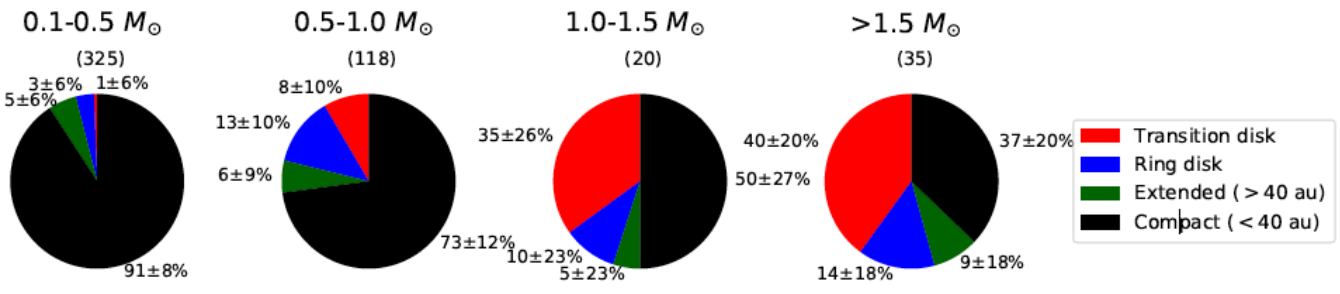

Figure 6. Distribution of disk morphologies for different stellar mass bins. Different disk morphologies are marked in red (transition disk), blue (ring disk), green (extended disks) and black (compact). The numbers in brackets above each pie chart indicate the number of targets in that stellar mass bin.

A deuterium-poor water reservoir in the asteroid 4 Vesta and the inner solar system

Stephant, A.; Wadhwa, M.; Hervig, R.; Bose, M.; Zhao, X.; Barrett, T. J.; Anand, M.; Franchi, I. A.

Geochimica et Cosmochimica Acta, Volume 297

Recent investigations of meteorites thought to originate from the asteroid 4 Vesta have suggested an early accretion of water on rocky bodies in the inner Solar System from a carbonaceous chondrite-like source. However, these studies have been based on the hydrogen isotope compositions (δD) of late-crystallizing apatite grains in eucrites that likely do not record the primary magmatic composition. We have determined the δD and H_2O concentrations in some of the earliest-formed silicates (clinopyroxenes) from several eucrites with the goal of constraining the hydrogen isotope composition of their source reservoir on their parent body. The H_2O concentrations in clinopyroxenes from eucrites Juvinas, Stannern and Tirhert range from 5 to 18 μg/g, with a weighted average δD of -263 ± 70‰. Their apatites and whitlockites exhibit a higher weighted average δD of -165 ± 73‰, possibly as a result of H2 degassing during or after phosphate crystallization. Thermal metamorphism of these eucrites has most probably resulted in the loss of H, and an increase in their original δD values. While the weighted average δD value for the eucrite clinopyroxenes reported here is inferred to reflect an upper limit for the isotopic composition of the silicate mantle reservoir on their parent asteroid 4 Vesta, the average δD value of Stannern clinopyroxenes is considered to be closest to the initial δD of the source mantle (i.e., -373 ± 127‰), which is lighter than that of Earth's depleted upper mantle and most carbonaceous chondrites. We suggest that at least some of the water in 4 Vesta (and possibly other rocky bodies in the inner Solar System) was derived from a relatively deuterium-poor reservoir in the protosolar nebula, which was incorporated into planetesimals formed early in Solar System history.

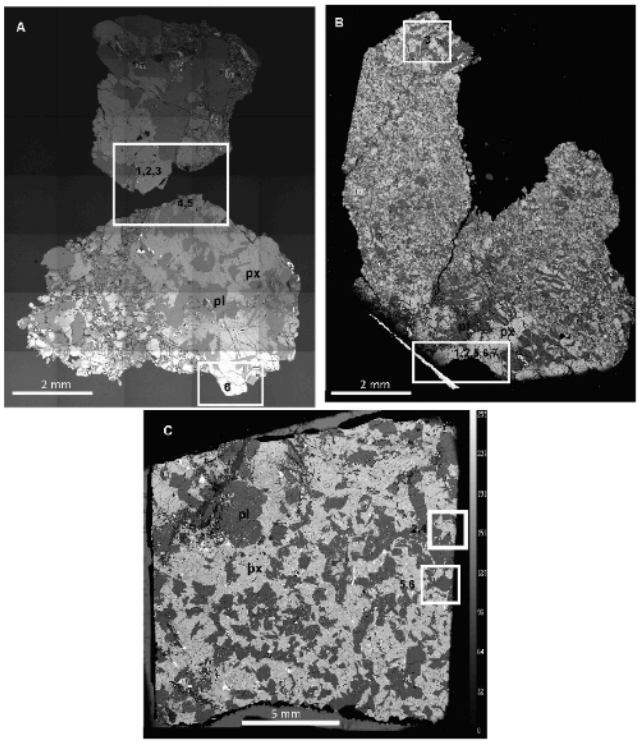

Fig. 1. Backscattered electron images of Juvinas (top left), Stannern (top right), Tirhert (bottom) thin sections. The scale bar is noted at the bottom left of each image.

Lithologic Controls on Silicate Weathering Regimes of Temperate Planets

Kaustubh Hakim, Dan J. Bower, Meng Tian, Russell Deitrick, Pierre Auclair-Desrotour, Daniel Kitzmann, Caroline Dorn, Klaus Mezger and Kevin Heng

The Planetary Science Journal, Volume 2, Number 2

Weathering of silicate rocks at a planetary surface can draw down CO2 from the atmosphere for eventual burial and long-term storage in the planetary interior. This process is thought to provide essential negative feedback to the carbonate-silicate cycle (carbon cycle) to maintain clement climates on Earth and potentially similar temperate exoplanets. We implement thermodynamics to determine weathering rates as a function of surface lithology (rock type). These rates provide upper limits that allow the maximum rate of weathering in regulating climate to be estimated. This modeling shows that the weathering of mineral assemblages in a given rock, rather than individual minerals, is crucial to determine weathering rates at planetary surfaces. By implementing a fluid-transport-controlled approach, we further mimic chemical kinetics and thermodynamics to determine weathering rates for three types of rocks inspired by the lithologies of Earth's continental and oceanic crust, and its upper mantle. We find that thermodynamic weathering rates of a continental crust-like lithology are about one to two orders of magnitude lower than those of a lithology characteristic of the oceanic crust. We show that when the CO2 partial pressure decreases or surface temperature increases, thermodynamics rather than kinetics exerts a strong control on weathering. The kinetically and thermodynamically limited regimes of weathering depend on lithology, whereas the supply-limited weathering is independent of lithology. Our results imply that the temperature sensitivity of thermodynamically limited silicate weathering may instigate a positive feedback to the carbon cycle, in which the weathering rate decreases as the surface temperature increases.

Thresholds for Particle Clumping by the Streaming Instability

Li, Rixin; Youdin, Andrew

Submitted to AAS Journals

The streaming instability (SI) is a mechanism to aerodynamically concentrate solids in protoplanetary disks and trigger the formation of planetesimals. The SI produces strong particle clumping if the ratio of solid to gas surface density -- an effective metallicity -- exceeds a critical value. This critical value depends on particle sizes and disk conditions such as radial drift-inducing pressure gradients and levels of turbulence. To quantify these thresholds, we perform a suite of vertically-stratified SI simulations over a range of dust sizes and metallicities. We find a critical metallicity as low as 0.4% for the optimum particle sizes and standard radial pressure gradients (normalized value of Π=0.05). This sub-Solar metallicity is lower than previous results due to improved numerical methods and computational effort. We discover a sharp increase in the critical metallicity for small solids, when the dimensionless stopping time (Stokes number) is ≤0.01. We provide simple fits to the size-dependent SI clumping threshold, including generalizations to different disk models and levels of turbulence. We also find that linear, unstratified SI growth rates are a surprisingly poor predictor of particle clumping in non-linear, stratified simulations, especially when the finite resolution of simulations is considered. Our results widen the parameter space for the SI to trigger planetesimal formation.

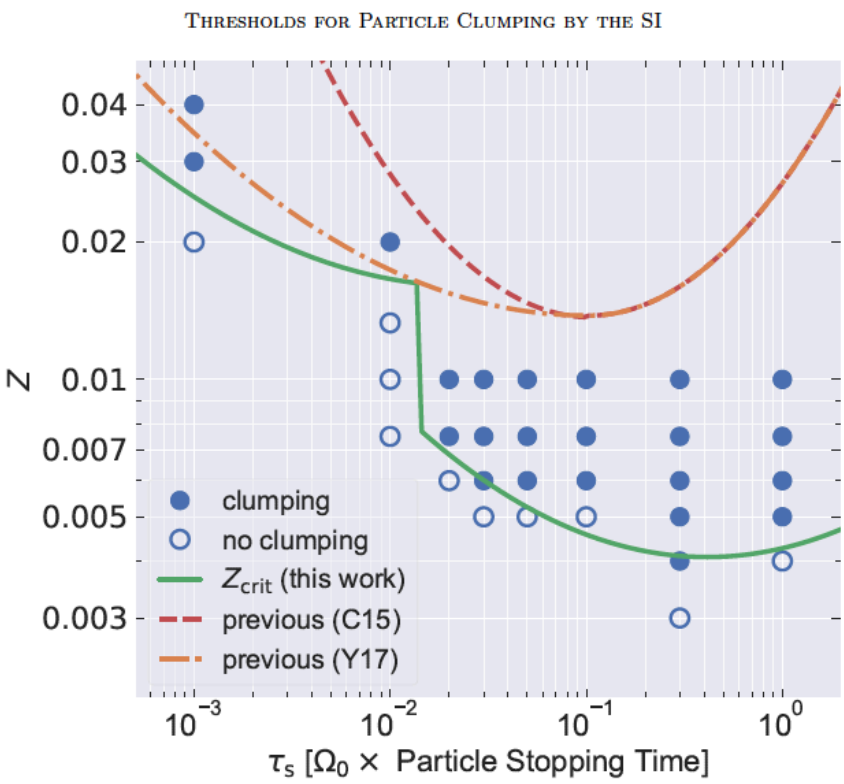

Figure 1. Overview of particle clumping by the SI for runs of different stopping times, s, and metallicities, *Z*, with radial pressure gradients set by = 0:05, and no additional sources of turbulence. Strong clumping occurs (or does not occur) for cases with filled (or open) circles. The minimum Z for strong clumping is fit by the *solid curve*. Previous boundaries are shown by the *dashed* and *dash-dotted* curves. See text for additional discussion including generalizations of the clumping boundary in Section 3.3. Table 1 gives additional simulation details. An interactive version of this plot with detailed analysis of each simulation is available at https://rixinli.com/tauZmap.html.

System-level fractionation of carbon from disk and planetesimal processing

Tim Lichtenberg, Sebastiaan Krijt

Accepted for publication in The Astrophysical Journal Letters

Finding and characterizing extrasolar Earth analogs will rely on interpretation of the planetary system's environmental context. The total budget and fractionation between C-H-O species sensitively affect the climatic and geodynamic state of terrestrial worlds, but their main delivery channels are poorly constrained. We connect numerical models of volatile chemistry and pebble coagulation in the circumstellar disk with the internal compositional evolution of planetesimals during the primary accretion phase. Our simulations demonstrate that disk chemistry and degassing from planetesimals operate on comparable timescales and can fractionate the relative abundances of major water and carbon carriers by orders of magnitude. As a result, individual planetary systems with significant planetesimal processing display increased correlation in the volatile budget of planetary building blocks relative to no internal heating. Planetesimal processing in a subset of systems increases the variance of volatile contents across planetary systems. Our simulations thus suggest that exoplanetary atmospheric compositions may provide constraints on *when* a specific planet formed.

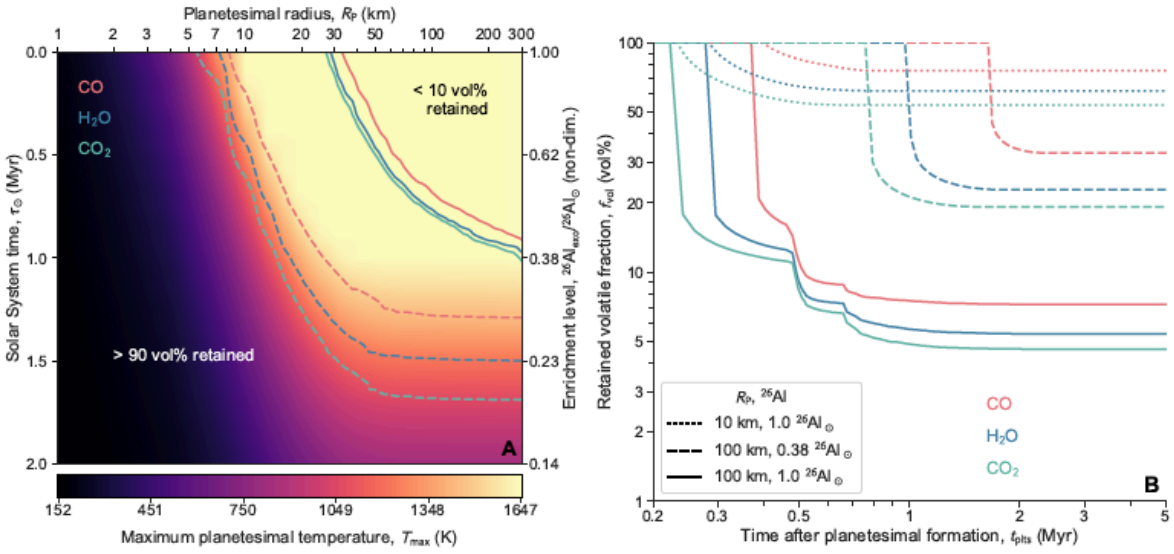

Figure 2. Thermal evolution of planetesimals and loss of H_2O, CO_2, and CO. (*Left*) Peak temperatures in the interior of planetesimals from radioactive decay of ^{26}Al (background color), interpolated from a grid of planetesimal simulations. The y-axes show enrichment level at the time of planetesimal formation ($^{26}Al_{exo}/^{26}Al_\odot$) and time after CAI formation in the Solar System. The x-axis (top) gives the radius of planetesimals. Colored lines indicate the retention of > 90 vol% (dashed) or 10 vol% (solid) of H_2O (blue), CO_2 (green), and CO (red) after peak heating inside the planetesimal. (*Right*) Loss of H_2O (blue), CO_2 (green), and CO (red) over time for different combinations of ^{26}Al abundance and planetesimal radius.

Blog post by Tim Lichtenberg